IET Optoelectronics

Research Article

IET Journals
The Institution of Engineering and Technology

Performance analysis of a novel hybrid FSO/RF communication system

ISSN 1751-8768
Received on 22nd December 2018
Revised 21st June 2019
Accepted on 17th September 2019
E-First on 23rd January 2020
doi: 10.1049/iet-opt.2018.5172
www.ietdl.org

Mohammad Ali Amirabadi[1] ✉, *Vahid Tabataba Vakili*[1]

[1]*School of Electrical Engineering, Iran University of Science and Technology, Tehran, Iran*

✉ *E-mail: m_amirabadi@elec.iust.ac.ir*

Abstract: In this paper, a novel dual-hop relay-assisted hybrid Free Space Optical / Radio Frequency (FSO / RF) communication system is presented. In this structure an access point connects users within the building to the Base Station via a hybrid parallel FSO / RF link, this link is proposed firstly. The parallel combination of FSO and RF links and use of an access point will increase capacity, reliability and data rate of the system. It is the first time that the effect of the number of users on the performance of a dual-hop relay-assisted hybrid parallel FSO / RF system is investigated. FSO link is considered in Gamma-Gamma atmospheric turbulence with the effect of pointing error and RF link is considered in Rayleigh fading. For the first time, closed-form expressions are derived for Bit Error Rate (BER) and Outage Probability (P_{out}) of the proposed system. Derived expressions are verified through MATLAB simulations. It is shown that performance of the proposed system is almost independent of atmospheric turbulence intensity, thereby when atmospheric turbulence strengthens, low power consumption is required for performance maintenance. Hence the proposed structure is suitable for mobile systems in which a small battery supplies transmitter power.

1 Introduction

According to the data traffic increase in modern communication systems, it is predicted that the fifth-generation cellular networks, in comparison with the fourth generation, requires 1000 times more capacity, ten times more spectral (energy) efficiency, 10–100 times more data rate, and 25 times more average cell throughput. Ultra-dense cellular network, with a large number of small cells, is one of the proposed solutions to increase the capacity. The data traffic of small cells is transmitted to the core through a backup network. Combination of the optical fibre link and millimetre-wave radiofrequency (RF) link is a good candidate for such a backup network. However, in ultra-dense cellular networks, RF interference is a problematic issue and also the capacity of millimetre-wave RF link is not enough for the requirements of the fifth-generation cellular network. Also, optical fibre has a high installation cost. Free-space optical (FSO) link has bandwidth and data rate equal to optical fibre link, and therefore, in hybrid structures, it is better to replace the optical fibre by FSO link [1].

FSO link is sensitive to atmospheric turbulence and weather conditions. Also, the effect of pointing error, which is caused by transceiver misalignment, significantly degrades the performance of the FSO system. Weather conditions apply constant loss on the received signal intensity, but atmospheric turbulence and pointing error lead to random fluctuations of the received signal intensity [2].

To investigate the effects of atmospheric turbulence, various statistical models have been presented in papers. Among them, log-normal, gamma–gamma, and negative exponential models are, respectively, in high compliance with experimental results, for weak, moderate-to-strong, and saturate atmospheric turbulence regimes. Mostly, in FSO system, intensity modulation/direct detection is used, among coherent detections, heterodyne detection is a complex technique that overcomes the effect of thermal noise [3].

FSO system has unlicensed bandwidth, inherent security, and easy setup. Combining FSO and millimetre-wave RF links significantly increases data rate and reliability of the system. Several protocols have been proposed for data processing in relay-assisted hybrid FSO/RF systems, among them amplify and forward [4] and detect and forward [5] are mostly used. In the amplify and forward protocol, amplification gain is fixed or adaptive. Fixed gain has less complexity, but more power dissipation, thereby it is better to be used only when channel state information (CSI) is unknown. When CSI is known, detection and forward, due to its low-power consumption is preferred.

In this work, the FSO link is considered at gamma–gamma atmospheric turbulence because this model is highly accompanied by experimental results. Also, to get closer to actual operations, the effect of pointing error is considered at FSO link. RF link is at Rayleigh fading. In this paper, two cases of known CSI and unknown CSI at the access point are considered. In the case of known CSI, received signal at the access point is detected, regenerated, and then forwarded. In the case of unknown CSI, received signal at the access point is amplified with fixed gain and forwarded. For the first time, closed-form expressions are derived for bit error rate (BER) and P_{out} of the proposed structure. Hybrid parallel FSO/RF structure significantly improves link accessibility and reliability as well as data rate; also, the use of an access point improves the capacity of the system; hence, the proposed structure will reduce power consumption while maintaining the performance of the system.

Rest of this paper is organised as follows: In Section 2, system model is described. Sections 3 and 4 investigate the performance of known CSI and unknown CSI schemes, respectively. Section 5 compares simulation and analytical results and brings some discussion. Section 6 is the conclusion of this work.

1.1 Related works

The investigations in the field of hybrid FSO/RF systems could be divided into three main categories. The first category investigates single-hop structure [6–14], which is composed of a parallel FSO/RF link and improves reliability and data rate. In this structure, either both FSO and RF links are active or FSO link is active and RF link acts as the backup link [11]. It was worth mentioning that multi-user [6] and received diversity [12] scenarios are also considered in some investigation of this category. The second category investigates dual-hop structure [15–37], which uses one relay station between source and destination, and improves capacity and reduces the total power consumption of the system. The third category investigates multi-hop structure [38–

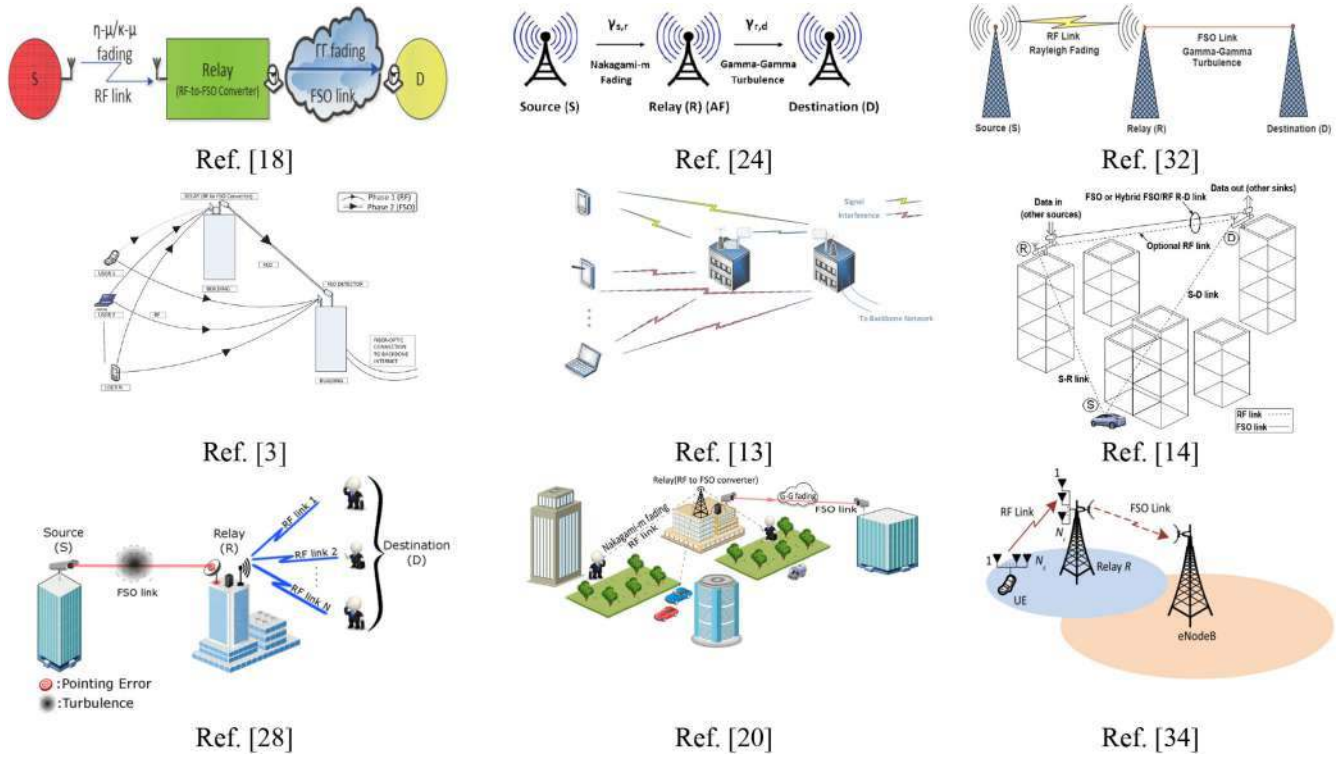

Fig. 1 *Main categories of dual-hop relay-assisted hybrid FSO/RF system: without backup (first row), with backup (second row), and multi-user (third row)*

43], which uses multiple relay stations between source and destination, and improves throughput of the system.

The dual-hop structure (the second category) could be divided into four sub-categories. The first sub-category considers a direct link (a backup connection) between source and destination [3, 4, 5, 15–24], and the second category does not consider this link [3, 15, 20–22, 24–35]. The third sub-category considers single-user scenario [16, 17, 20, 23, 24, 25, 27, 30, 31, 33–35], and the fourth sub-category considers multi-user scenario [3, 15, 21, 24, 26, 28, 29, 32].

The gamma–gamma distribution is mostly used for modelling atmospheric turbulence, because it is highly accompanied with the actual results for weak-to-strong atmospheric turbulence regimes [3, 15–17, 20, 22, 23, 25–31, 33–35]. However, some works considered M [24, 32, 36, 37], exponential Weibull [21], and alpha–mu [18] distributions. The Rayleigh distribution is mostly used for modelling the fading of line of sight links [3, 16, 20, 24, 27, 31, 33–35], and the Nakagami-m distribution is mostly used for modelling the fading of multi-path links [15, 20–22, 25, 28–30], because they are highly accompanied with the actual results. However, few works considered Rician distribution [26].

According to the above literature review, and according to the best of authors' knowledge, the novelties and contributions of this work (compared with the dual-hop hybrid FSO/RF systems) include: (i) considering a parallel FSO/RF link, (ii) considering opportunistic channel allocation scenario for the multi-user scenario, (iii) investigating the effect of number of users on the performance of the system, (iv) considering wide range of atmospheric turbulences, from moderate to saturate, and (v) considering two different relaying protocols.

To further clarify the contributions and novelties of this work, the most similar dual-hop hybrid FSO/RF systems are exactly copied from their references and pasted in Fig. 1. As can be seen in Fig. 1 and the main text of references, none of these references considered subjects such as parallel FSO/RF link, two different relaying protocols, wide range of atmospheric turbulences, and the effect of number of users.

2 System model

Consider a practical application: assume that there are some users in a building (e.g. workers of a company), they want to connect (with their mobiles) to the base station (e.g. for checking Internet). In this situation, users are inside (in the building), and the base station is outside (in the free space). They are frequently encountered with bad communication channel condition (sometimes channel is bad for FSO link and sometimes for RF link). What is the best idea for helping them? You know, some people living in some climates such as the Mediterranean are always encountered with this. Generally speaking increasing power consumption or adding processing or coding etc. is not a good idea for mobile communication that the transmitter is supplied by a small mobile battery and the user, expect this battery to serve at least for some days. The best idea is to use a relay; in addition, parallelising FSO and RF links would solve the problem of bad channel condition (because FSO and RF are complements of each other).

The whole system is not in a building: the access point (which is on the roof) is connected to multiple RF users (which are in the building) and the access point, through a parallel hybrid FSO/RF link, is connected to the base station (which is out of the building). Multiple users are in a building, but in each time slot, only one of them could be connected to the base station; therefore, a user with best channel condition is selected. The dual-hop hybrid FSO/RF communication system of Fig. 2 is considered, where mobile users communicate with the destination via the intermediate access point by adopting amplify and forward or detect and forward relaying schemes.

Let $x_{1,\,i}$; $i = 1, 2, \ldots, N$ be the transmitted RF signal from the ith user to access point through RF link. The received signal at the access point is expressed as

$$y_{1,\,i} = h_i x_{1,\,i} + e_{1,\,i}, \tag{1}$$

where h_i represents the fading coefficient of the RF link between the ith user and the access point and $e_{1,\,i}$ represents the additive white Gaussian noise (AWGN) at access point input with the variance of σ^2_{RF} and zero mean.

Received signal with the highest signal-to-noise ratio (SNR) is selected at the access point. Instantaneous SNR at the access point input is written as

$$\gamma_1 = \max\left(\gamma_{1,\,1}, \gamma_{1,\,2}, \ldots, \gamma_{1,\,N}\right). \tag{2}$$

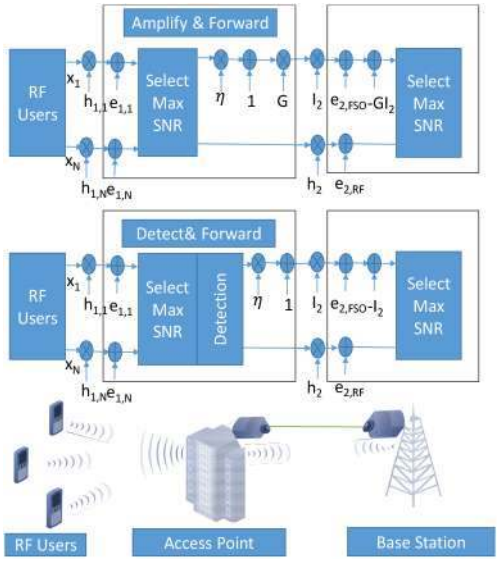

Fig. 2 *Proposed relay-assisted hybrid FSO/RF system*

The common transmission rate of FSO system is in the order of 10 Gbit/s; according to that in the proposed system, additional coding or processing or special transmission structure that could affect the transmission rate is not used, the rate of this system would remain as 10 Gbit/s. The proposed structure is presented for a mobile communication scenario, which is encountered by bad communication channel condition. The point that this system is used for mobile users that want to communicate with base station clarifies that the link is not so long. Since common mobile-base station links are below 1 km (it is dependent on population density).

In this system, in the case of known CSI, the received RF signal with the highest SNR at the access point input is detected, regenerated, then two copies of the generated signal are forwarded through parallel FSO and RF links. At the FSO link, the RF signal is first converted to FSO by conversion efficiency of η, then a direct current (DC) bias is added to ensure that the FSO signal is non-negative. Transmitted FSO and RF signals are as follows:

$$x_{2,\,\mathrm{FSO}} = 1 + \eta d_1, \tag{3}$$

$$x_{2,\,\mathrm{RF}} = d_1, \tag{4}$$

where d_1 is the regenerated signal. The transmitted signal is affected by channel atmospheric turbulence and receiver input noise. Finally, after DC removal from FSO signal, received FSO and RF signals at the base station are given by

$$y_{2,\,\mathrm{FSO}} = I_2 x_{2,\,\mathrm{FSO}} + e_{2,\,\mathrm{FSO}} - I_2 = I_2 \eta d_1 + e_{2,\,\mathrm{FSO}}, \tag{5}$$

$$y_{2,\,\mathrm{RF}} = h_2 x_{2,\,\mathrm{RF}} + e_{2,\,\mathrm{RF}} = h_2 d_1 + e_{2,\,\mathrm{RF}}, \tag{6}$$

where I_2 is atmospheric turbulence intensity along with FSO link, $e_{2,\,\mathrm{FSO}}$ represents the AWGN with zero mean and variance of σ^2_{FSO} at the FSO receiver input, h_2 is the RF fading coefficient, and $e_{2,\,\mathrm{RF}}$ is AWGN with zero mean and variance of σ^2_{RF} at the RF receiver input.

In the case of unknown CSI, the received RF signal with the highest SNR at the access point input is selected, amplified with fixed gain, then two copies of it are forwarded through parallel FSO and RF links as

$$x_{2,\,\mathrm{FSO}} = G(1 + \eta y_1), \tag{7}$$

$$x_{2,\,\mathrm{RF}} = G y_1, \tag{8}$$

where y_1 is the selected signal. Received FSO and RF signals at the base station are given by

$$y_{2,\,\mathrm{FSO}} = I_2 x_{2,\,\mathrm{FSO}} + e_{2,\,\mathrm{FSO}} - G I_2 = G\eta I_2 y_1 + e_{2,\,\mathrm{FSO}}, \tag{9}$$

$$y_{2,\,\mathrm{RF}} = h_2 x_{2,\,\mathrm{RF}} + e_{2,\,\mathrm{RF}} = G h_2 y_1 + e_{2,\,\mathrm{RF}}. \tag{10}$$

Assuming transmitted signal with unit energy, the instantaneous SNRs at base station receivers input are as follows:

$$\gamma_{\mathrm{FSO}} = \frac{G^2\eta^2 I_2^2 h_1^2}{G^2\eta^2 I_2^2 \sigma^2_{\mathrm{RF}} + \sigma^2_{\mathrm{FSO}}}, \tag{11}$$

$$\gamma_{\mathrm{RF}} = \frac{G^2\eta^2 h_2^2 h_1^2}{G^2 h_2^2 \sigma^2_{\mathrm{RF}} + \sigma^2_{\mathrm{RF}}}. \tag{12}$$

Regarding the fixed-gain relay strategy at the unknown CSI scheme, its gain is fixed to a constant value, which is independent of the CSI of the first-hop channel. The amplification gain is fixed to $G^2 = 1/(C\sigma^2_{\mathrm{RF}})$, where C is a constant parameter. Defining $\gamma_1 = h_1^2/\sigma^2_{\mathrm{RF}}$, $\gamma_{2,\,\mathrm{RF}} = G^2 h_2^2/\sigma^2_{\mathrm{RF}}$ and $\gamma_{2,\,\mathrm{FSO}} = G^2\eta^2 I_2^2/\sigma^2_{\mathrm{FSO}}$, instantaneous SNR at the base station receivers input becomes as follows:

$$\gamma_{\mathrm{FSO}} = \frac{\gamma_1 \gamma_{2,\,\mathrm{FSO}}}{\gamma_{2,\,\mathrm{FSO}} + C}, \tag{13}$$

$$\gamma_{\mathrm{RF}} = \frac{\gamma_1 \gamma_{2,\,\mathrm{RF}}}{\gamma_{2,\,\mathrm{RF}} + C}. \tag{14}$$

Since the amplification gain is fixed, the forwarded signal has varying output power, due to the effect of the channel fading by the first hop before their fixed-gain amplification. At the base station, between received FSO and RF signals, signal with higher SNR is selected for detection. Therefore, instantaneous SNR at the base station receiver input is as follows:

$$\gamma_2 = \max(\gamma_{\mathrm{FSO}}, \gamma_{\mathrm{RF}}). \tag{15}$$

In the present paper, the FSO link is investigated in a wide range of atmospheric turbulence regimes, from moderate to strong. The best model that accompanies experimental results of this range is gamma–gamma distribution. Also, the effect of pointing error is considered to get closer to actual results. Cumulative distribution function (CDF) of gamma–gamma atmospheric turbulence with the effect of pointing error is as follows [43]:

$$F_\gamma(\gamma) = \frac{\xi^2}{\Gamma(\alpha)\Gamma(\beta)} G_{2,\,4}^{3,\,1}\left(\alpha\beta\kappa\sqrt{\frac{\gamma}{\bar{\gamma}_{\mathrm{FSO}}}}\,\middle|\,\begin{matrix}1,\ \xi^2+1\\ \xi^2,\ \alpha,\ \beta,\ 0\end{matrix}\right), \tag{16}$$

where $G_{p,q}^{m,n}\left(z\middle|\begin{matrix}a_1, a_2, \ldots, a_p\\ b_1, b_2, \ldots, b_q\end{matrix}\right)$ is the Meijer-G function [44, Eq. 07.34.02.0001.01] 0, $\Gamma(.)$ is well known gamma function [44, Eq. 06.05.02.0001.01] $\alpha = \left[\exp\left(0.49\sigma_R^2/\left(1+1.11\sigma_R^{12/5}\right)^{7/6}\right)-1\right]^{-1}$ and $\beta = \left[\exp\left(0.51\sigma_R^2/\left(1+0.69\sigma_R^{12/5}\right)^{5/6}\right)-1\right]^{-1}$ are parameters related to gamma–gamma atmospheric turbulence, where σ_R^2 is Rytov variance, and $\xi^2 = \omega_{Z_{eq}}/(2\sigma_s)$ is the ratio of the equivalent received beam radius to the standard deviation of pointing errors at the receiver [45]. $\bar{\gamma}_{FSO} = \eta^2/\sigma_{FSO}^2$ represents average SNR at the FSO receiver input.

In an urban environment, the RF transmission links spanning are subjected to multi-path fading, which can be characterised by Rayleigh distribution [23]. Accordingly, the instantaneous SNR of the RF link obeys an exponential distribution with the following probability density function (PDF) and CDF:

$$f_\gamma(\gamma) = \frac{1}{\bar{\gamma}_{RF}} e^{-(\gamma/\bar{\gamma}_{RF})}, \tag{17}$$

$$F_\gamma(\gamma) = 1 - e^{-(\gamma/\bar{\gamma}_{RF})}, \tag{18}$$

where $\bar{\gamma}_{RF} = 1/\sigma_{RF}^2$ is average SNR at the RF receiver input. According to (2), the CDF of γ_1 random variable becomes as follows:

$$\begin{aligned} F_{\gamma_1}(\gamma) &= \Pr\left(\max\left(\gamma_{1,1}, \gamma_{1,2}, \ldots, \gamma_{1,N}\right) \le \gamma\right) \\ &= \Pr\left(\gamma_{1,1} \le \gamma, \gamma_{1,2} \le \gamma, \ldots, \gamma_{1,N} \le \gamma\right). \end{aligned} \tag{19}$$

Assuming independent and identically distributed RF paths and using (18), CDF of γ_1 random variable becomes as follows:

$$\begin{aligned} F_{\gamma_1}(\gamma) &= \prod_{i=1}^{N} \Pr\left(\gamma_{1,i} \le \gamma\right) = \prod_{i=1}^{N} F_{\gamma_{1,i}}(\gamma) \\ &= \left(F_{\gamma_{1,i}}(\gamma)\right)^N = \left(1 - e^{-(\gamma/\bar{\gamma}_{RF})}\right)^N. \end{aligned} \tag{20}$$

Differentiating the above equation, the PDF of γ_1 random variable becomes as follows:

$$\begin{aligned} f_{\gamma_1}(\gamma) &= N\left(F_{\gamma_{1,i}}(\gamma)\right)^{N-1} f_{\gamma_{1,i}}(\gamma) \\ &= \frac{N}{\bar{\gamma}_{RF}}\left(1 - e^{-(\gamma/\bar{\gamma}_{RF})}\right)^{N-1} e^{-(\gamma/\bar{\gamma}_{RF})}. \end{aligned} \tag{21}$$

Substituting binomial expansion of $\left(1 - e^{-(\gamma/\bar{\gamma}_{RF})}\right)^{N-1}$ as $\sum_{k=0}^{N-1}\binom{N-1}{k}(-1)^k e^{-(k\gamma/\bar{\gamma}_{RF})}$, the PDF of γ_1 random variable becomes as follows:

$$f_{\gamma_1}(\gamma) = \sum_{k=0}^{N-1}\binom{N-1}{k}(-1)^k \frac{N}{\bar{\gamma}_{RF}} e^{-((k+1)\gamma/\bar{\gamma}_{RF})}. \tag{22}$$

According to (15), the CDF of γ_1 random variable becomes as follows:

$$\begin{aligned} F_{\gamma_2}(\gamma) &= \Pr\left(\max\left(\gamma_{FSO}, \gamma_{RF}\right) \le \gamma\right) \\ &= \Pr\left(\gamma_{FSO} \le \gamma, \gamma_{RF} \le \gamma\right). \end{aligned} \tag{23}$$

3 Performance of known CSI scheme

Under the idealised simplifying assumption of having perfect CSI, modulation with coherent detection requires lower SNR than their non-coherent detection counterparts. However, the phase recovery error degrades the performance of the system with coherent detection, while differential detections such as differential phase shift keying (DPSK) are less sensitive to it. Practically, non-coherent modulations are better choices due to the carrier synchronisation and the carrier recovery error. Moreover, non-coherent detection also reduces the complexity of the receiver [23]. In this work, the BER and P_{out} of DPSK and are investigated analytically.

3.1 Outage probability

Given that $P_{out}(\gamma_{th}) = F_\gamma(\gamma_{th})$, and assuming that error occurs only due to the error of the access point and base station receivers, for the proposed detect and forward scheme, P_{out} is given by [46]

$$\begin{aligned} P_{out}(\gamma_{th}) &= \cup_{j=1}^{2}\left(\Pr\left\{j\text{th link is in outage}\right\}\right) \\ &= 1 - \cap_{j=1}^{2}\left(\Pr\left\{j\text{th link is avalable}\right\}\right) \\ &= 1 - \left[1 - P_{out,1}(\gamma_{th})\right]\left[1 - P_{out,2}(\gamma_{th})\right] \\ &= 1 - \left[1 - F_{\gamma_1}(\gamma_{th})\right]\left[1 - F_{\gamma_2}(\gamma_{th})\right]. \end{aligned} \tag{24}$$

Assuming independent FSO and RF links, substituting (16), (18), and (20) into (24), P_{out} of the proposed structure is calculated as follows: (see (25)) . Substituting binomial expansion of $\left(1 - e^{-(\gamma_{th}/\bar{\gamma}_{RF})}\right)^N$ in (25), P_{out} of the proposed structure becomes as follows:

$$\begin{aligned} P_{out}(\gamma_{th}) = &\sum_{k=0}^{N}\binom{N}{k}(-1)^k e^{-(k\gamma_{th}/\bar{\gamma}_{RF})} \\ &+ \frac{\xi^2}{\Gamma(\alpha)\Gamma(\beta)}\left(1 - e^{-(\gamma_{th}/\bar{\gamma}_{RF})}\right) G_{2,4}^{3,1}\left(\alpha\beta\kappa\sqrt{\frac{\gamma_{th}}{\bar{\gamma}_{FSO}}}\middle|\begin{matrix}1, \xi^2+1\\ \xi^2, \alpha, \beta, 0\end{matrix}\right) \\ &- \sum_{k=0}^{N}\binom{N}{k}(-1)^k \frac{\xi^2}{\Gamma(\alpha)\Gamma(\beta)}\left(e^{-(k\gamma_{th}/\bar{\gamma}_{RF})} - e^{-((k+1)\gamma_{th}/\bar{\gamma}_{RF})}\right) \\ &\times G_{2,4}^{3,1}\left(\alpha\beta\kappa\sqrt{\frac{\gamma_{th}}{\bar{\gamma}_{FSO}}}\middle|\begin{matrix}1, \xi^2+1\\ \xi^2, \alpha, \beta, 0\end{matrix}\right). \end{aligned} \tag{26}$$

3.2 Bit error rate

BER of DPSK modulation is calculated analytically from the following equation [12]:

$$P_e = \frac{1}{2}\int_0^\infty e^{-\gamma} F_\gamma(\gamma)\,d\gamma = \frac{1}{2}\int_0^\infty e^{-\gamma} P_{out}(\gamma)\,d\gamma. \tag{27}$$

(see (28))

Substituting (26) into (27) and using [44, Eq. 07.34.21.0088.01], BER of DPSK modulation becomes equal to (28), where $\varphi_1 = \left(0, \frac{1}{2}, 1, \frac{1+\xi^2}{2}, \frac{2+\xi^2}{2}\right)$ and $\varphi_2 = \left(\frac{\xi^2}{2}, \frac{1+\xi^2}{2}, \frac{\alpha}{2}, \frac{1+\alpha}{2}, \frac{\beta}{2}, \frac{1+\beta}{2}, 0, \frac{1}{2}\right)$.

4 Performance of unknown CSI scheme

According to (13), the CDF of the γ_{FSO} random variable is as follows:

$$\begin{aligned} P_{out}(\gamma_{th}) = 1 - &\left[1 - \left(1 - e^{-(\gamma_{th}/\bar{\gamma}_{RF})}\right)^N\right] \\ &\times\left[1 - \frac{\xi^2}{\Gamma(\alpha)\Gamma(\beta)}\left(1 - e^{-(\gamma_{th}/\bar{\gamma}_{RF})}\right) G_{2,4}^{3,1}\left(\alpha\beta\kappa\sqrt{\frac{\gamma_{th}}{\bar{\gamma}_{FSO}}}\middle|\begin{matrix}1, \xi^2+1\\ \xi^2, \alpha, \beta, 0\end{matrix}\right)\right]. \end{aligned} \tag{25}$$

$$F_{\gamma\mathrm{FSO}}(\gamma) = \Pr(\gamma_{\mathrm{FSO}} \le \gamma) = 1 - \Pr(\gamma_{\mathrm{FSO}} \ge \gamma) = 1 - \Pr\left(\frac{\gamma_1\gamma_{2,\mathrm{FSO}}}{\gamma_{2,\mathrm{FSO}} + C} \ge \gamma\right). \tag{29}$$

After mathematical simplification, (29) becomes as follows [26]:

$$F_{\gamma\mathrm{FSO}}(\gamma) = 1 - \int_0^{\infty} \Pr\left(\gamma_{2,\mathrm{FSO}} \ge \frac{\gamma C}{x}\middle|\gamma_1\right) f_{\gamma_1}(\gamma + x)\mathrm{d}x. \tag{30}$$

Substituting (16) and (22) into (30) obtains:

$$F_{\gamma\mathrm{FSO}}(\gamma) = 1 - \sum_{k=0}^{N-1}\binom{N-1}{k}(-1)^k \frac{N}{\bar{\gamma}_{\mathrm{RF}}} \mathrm{e}^{-((k+1)\gamma/\bar{\gamma}_{\mathrm{RF}})} \times \left[\int_0^{\infty} \mathrm{e}^{-((k+1)x/\bar{\gamma}_{\mathrm{RF}})}\mathrm{d}x - \frac{\xi^2}{\Gamma(\alpha)\Gamma(\beta)} \times \int_0^{\infty} \mathrm{e}^{-((k+1)x/\bar{\gamma}_{\mathrm{RF}})} G_{2,4}^{3,1}\left(\alpha\beta\kappa\sqrt{\frac{\gamma C}{x\bar{\gamma}_{\mathrm{FSO}}}}\middle|\begin{matrix}1,\ \xi^2+1\\ \xi^2,\ \alpha,\ \beta,\ 0\end{matrix}\right)\mathrm{d}x\right]. \tag{31}$$

Substituting equivalent Meijer-G of $G_{2,4}^{3,1}\left(\alpha\beta\kappa\sqrt{\gamma C/x\bar{\gamma}_{\mathrm{FSO}}}\middle|\begin{matrix}1,\ \xi^2+1\\ \xi^2,\ \alpha,\ \beta,\ 0\end{matrix}\right)$ as $G_{4,2}^{1,3}\left(\frac{1}{\alpha\beta\kappa}\sqrt{x\bar{\gamma}_{\mathrm{FSO}}/\gamma C}\middle|\begin{matrix}1-\xi^2,\ 1-\alpha,\ 1-\beta,\ 1\\ 0,\ -\xi^2\end{matrix}\right)$ [44, Eq. 07.34.17.0012.01], and using [44, Eq. 07.34.21.0088.01], CDF of γ_{FSO} random variable becomes as follows: (see (32)) , where $\psi_1 = \left(1,\ \frac{1}{2},\ \frac{2+\xi^2}{2},\ \frac{1+\xi^2}{2}\right)$ and $\psi_2 = \left(1,\ \frac{1+\xi^2}{2},\ \frac{\xi^2}{2},\ \frac{1+\alpha}{2},\ \frac{\alpha}{2},\ \frac{1+\beta}{2},\ \frac{\beta}{2},\ \frac{1}{2},\ 0\right)$. According to (14), the CDF of γ_{RF} random variable is equal to

$$F_{\gamma\mathrm{RF}}(\gamma) = \Pr(\gamma_{\mathrm{RF}} \le \gamma) = 1 - \Pr(\gamma_{\mathrm{RF}} \ge \gamma) = 1 - \Pr\left(\frac{\gamma_1\gamma_{2,\mathrm{RF}}}{\gamma_{2,\mathrm{RF}} + C} \ge \gamma\right). \tag{33}$$

After mathematical simplification, the above statement comes as follows:

$$F_{\gamma\mathrm{RF}}(\gamma) = 1 - \int_0^{\infty} \Pr\left(\gamma_{2,\mathrm{RF}} \ge \frac{\gamma C}{x}\middle|\gamma_1\right) f_{\gamma_1}(\gamma + x)\mathrm{d}x. \tag{34}$$

Substituting (18) and (22) into (34) obtains

$$F_{\gamma\mathrm{RF}}(\gamma) = 1 - \int_0^{\infty} \mathrm{e}^{-(\gamma C/x\bar{\gamma}_{\mathrm{RF}})}\left(\frac{N}{\bar{\gamma}_{\mathrm{RF}}} \times \sum_{k=0}^{N-1}\binom{N-1}{k}(-1)^k \mathrm{e}^{-((k+1)(x+\gamma)/\bar{\gamma}_{\mathrm{RF}})}\right)\mathrm{d}x. \tag{35}$$

Substituting equivalent Meijer-G of $\mathrm{e}^{-(\gamma C/x\bar{\gamma}_{\mathrm{RF}})}$ as $G_{1,0}^{0,1}\left(\gamma C/x\bar{\gamma}_{\mathrm{RF}}\middle|\begin{matrix}1\\ -\end{matrix}\right)$ [44, Eq. 07.34.03.1081.01], (35) becomes:

$$F_{\gamma\mathrm{RF}}(\gamma) = 1 - \frac{N}{\bar{\gamma}_{\mathrm{RF}}}\sum_{k=0}^{N-1}\binom{N-1}{k} \times (-1)^k \mathrm{e}^{-((k+1)\gamma/\bar{\gamma}_{\mathrm{RF}})} \int_0^{\infty} \mathrm{e}^{-((k+1)x/\bar{\gamma}_{\mathrm{RF}})} G_{1,0}^{0,1}\left(\frac{\gamma C}{x\bar{\gamma}_{\mathrm{RF}}}\middle|\begin{matrix}1\\ -\end{matrix}\right)\mathrm{d}x. \tag{36}$$

Using [44, Eq. 07.34.17.0012.01] and [44, Eq. 07.34.21.0088.01], CDF of γ_{RF} random variable becomes equal to:

$$F_{\gamma\mathrm{RF}}(\gamma) = 1 - \sum_{k=0}^{N-1}\binom{N-1}{k}(-1)^k \frac{N}{k+1} \times \mathrm{e}^{-((k+1)\gamma/\bar{\gamma}_{\mathrm{RF}})} G_{0,2}^{2,0}\left(\frac{\gamma C(k+1)}{\bar{\gamma}_{\mathrm{RF}}^2}\middle|\begin{matrix}-\\ 1,\ 0\end{matrix}\right). \tag{37}$$

4.1 Outage probability

Given that $P_{\mathrm{out}}(\gamma_{\mathrm{th}}) = F_{\gamma}(\gamma_{\mathrm{th}})$, and using (15) and assuming independent FSO and RF links, P_{out} of unknown CSI scheme becomes as follows:

$$P_{\mathrm{out}}(\gamma_{\mathrm{th}}) = F_{\gamma_2}(\gamma_{\mathrm{th}}) = \Pr(\max(\gamma_{\mathrm{FSO}}, \gamma_{\mathrm{RF}}) \le \gamma_{\mathrm{th}}) = \Pr(\gamma_{\mathrm{FSO}} \le \gamma_{\mathrm{th}}, \gamma_{\mathrm{RF} \le \gamma_{\mathrm{th}}}) = P_{\mathrm{out,FSO}}(\gamma_{\mathrm{th}})P_{\mathrm{out,RF}}(\gamma_{\mathrm{th}}) \tag{38}$$

(see (39))
(see (40))

Substituting (32) and (37) into (38), and after some mathematical simplifications, P_{out} of the proposed structure of the CSI non-existence scheme becomes as (39).

From (38), $P_{\mathrm{out}} = P_{\mathrm{out,FSO}}P_{\mathrm{out,RF}}$, which means outage disrupts this link only when both FSO and RF links go in the outage. The relay of this structure is fixed gain, not adaptive, which means that even if one of the links disrupts, the system continues working without any attention; the main problem of this system is that it may also amplify noise. This is the physical reason for the mathematical complexity of (39) rather than the adaptive case of (26) because any physical phenomena affect this system and should

$$P_{\mathrm{e}} = \frac{1}{2}\left\{\sum_{k=0}^{N}\binom{N}{k}(-1)^k \frac{1}{1+(k/\bar{\gamma}_{\mathrm{RF}})} + \frac{\xi^2}{\Gamma(\alpha)\Gamma(\beta)} \times \left(G_{5,8}^{6,3}\left(\frac{(\alpha\beta\kappa)^2}{16\bar{\gamma}_{\mathrm{FSO}}}\middle|\begin{matrix}\varphi_1\\ \varphi_2\end{matrix}\right) - \frac{1}{1+(1/\bar{\gamma}_{\mathrm{RF}})}G_{5,8}^{6,3}\left(\frac{(\alpha\beta\kappa)^2}{16\bar{\gamma}_{\mathrm{FSO}}(1+(1/\bar{\gamma}_{\mathrm{RF}}))}\middle|\begin{matrix}\varphi_1\\ \varphi_2\end{matrix}\right)\right) - \sum_{k=0}^{N}\binom{N}{k}(-1)^k \frac{\xi^2}{\Gamma(\alpha)\Gamma(\beta)} \times \left(\frac{1}{1+(k/\bar{\gamma}_{\mathrm{RF}})}G_{5,8}^{6,3}\left(\frac{(\alpha\beta\kappa)^2}{16\bar{\gamma}_{\mathrm{FSO}}(1+(k/\bar{\gamma}_{\mathrm{RF}}))}\middle|\begin{matrix}\varphi_1\\ \varphi_2\end{matrix}\right) - \frac{1}{1+(k+1/\bar{\gamma}_{\mathrm{RF}})}G_{5,8}^{6,3}\left(\frac{(\alpha\beta\kappa)^2}{16\bar{\gamma}_{\mathrm{FSO}}(1+(k+1/\bar{\gamma}_{\mathrm{RF}}))}\middle|\begin{matrix}\varphi_1\\ \varphi_2\end{matrix}\right)\right)\right\} \tag{28}$$

$$F_{\gamma\mathrm{FSO}}(\gamma) = 1 - \sum_{k=0}^{N-1}\binom{N-1}{k}(-1)^k \frac{N}{k+1} \times \mathrm{e}^{-((k+1)\gamma/\bar{\gamma}_{\mathrm{RF}})}\left[1 - \frac{\xi^2 2^{\alpha+\beta-3}}{\pi\Gamma(\alpha)\Gamma(\beta)} G_{4,9}^{7,2}\left(\frac{(\alpha\beta\kappa)^2 C\gamma(k+1)}{16\bar{\gamma}_{\mathrm{FSO}}\bar{\gamma}_{\mathrm{RF}}}\middle|\begin{matrix}\psi_1\\ \psi_2\end{matrix}\right)\right], \tag{32}$$

be considered, while in (26) each part of the system was working independently due to the adaptive phenomena of the used relay.

4.2 Bit error rate

To derive BER, (39) should be inserted into (27) and integration should be solved. To solve this integration, first, the exp(.) term of the last summation of (39) [not the two first summations of (39)] should be substituted by its Meijer-G equivalent using [44, Eq. 07.34.03.1081.01], then the integration could be easily solved using [44, Eq. 07.34.21.0088.01] (for the first two summations) and [44, Eq. 07.34.21.0081.01] (for the last summation). Doing this procedure, the BER of DPSK modulation of CSI non-existence scheme becomes as (40), where $G_{p_1,\,q_1:p_2,\,q_2:p_3,\,q_3}^{n_1,\,m_1:n_2,\,m_2:n_3,\,m_3}\left(\begin{matrix}a_1,\,a_2,\,\ldots,\,a_{p_1}\\ b_1,\,b_2,\,\ldots,\,b_{q_1}\end{matrix}\middle|\begin{matrix}c_1,\,c_2,\,\ldots,\,c_{p_2}\\ d_1,\,d_2,\,\ldots,\,d_{q_2}\end{matrix}\middle|\begin{matrix}e_1,\,e_2,\,\ldots,\,e_{p_3}\\ f_1,\,f_2,\,\ldots,\,f_{q_3}\end{matrix}\middle|x,\,y\right)$ is the extended bivariate Meijer-G function [47].

It is correct that with modern computing tools, it is now easier to produce analytical expressions, and these may well be horrible as is the case here. However, it should be considered that the complexity of these formulations is related to the complex structure considered for the proposed system. In fact, if one uses modern computing tools, he could not get shorter forms of these formulations; since, its well known that Meijer-G form is the shortest possible closed-form expression one can find for any mathematical expressions. Moreover, its use as a tool in many of the well-cited papers published in FSO performance investigation.

The main attempt of this work is to present and investigate a new structure, as a solution to one of the most challenging problems in new communication systems, i.e. consumed power by the transmitter. This paper shows that a wide range of atmospheric turbulence even with the effect of pointing errors, it is possible to have a very good connection by consuming low power, without additional complexity or processing latency. It shows that there is no need to 'do' implement huge coding or heavy detection as well as complicated processing or massive antennas to make communication possible. That is the point; complexity is a non-dissociable part in most of the existing communication systems, and simplicity is something forgotten. Since they should serve the huge number of users with high reliability, rate, and performance, this is almost not possible without complexity. However, the proposed structure, only by the addition of one simple FSO transceiver, shows that it is possible. In this structure, the consumer does not require to consume more power or add more complexity, and the receiver does not need to implement additional processing or complicated detection, and this is a significant practical insight of this system.

5 Simulation results

In this section, theoretical analysis of the proposed hybrid FSO/RF system performance is compared with MATLAB simulation results, for both known CSI and unknown CSI schemes. FSO link has gamma–gamma atmospheric turbulence with the effect of pointing error and RF link has Rayleigh fading. For simplicity and without loss of generality, FSO and RF links are assumed to have equal average SNR $\left(\bar{\gamma}_{\mathrm{FSO}}=\bar{\gamma}_{\mathrm{RF}}=\gamma_{\mathrm{avg}}\right)$. Moderate $(\alpha=4,\ \beta=1.9,\ \xi=10.45)$ and strong $(\alpha=4.2,\ \beta=1.4,\ \xi=2.45)$ regimes of gamma–gamma atmospheric turbulence with the effect of pointing error are investigated. Also, it is assumed that $\eta=1$ and $C=1$.

In Fig. 3, outage probability of the proposed structure is plotted in terms of average SNR for moderate $(\alpha=4,\ \beta=1.9,\ \xi=10.45)$ and strong $(\alpha=4.2,\ \beta=1.4,\ \xi=2.45)$ atmospheric turbulence regimes, for both cases of known CSI and unknown CSI, number of users of $N=2$, and outage threshold SNR of $\gamma_{\mathrm{th}}=10\,\mathrm{dB}$. In both cases of known CSI and unknown CSI, there is little difference between system performance at moderate and strong regimes. For example, at $P_{\mathrm{out}}=10^{-2}$, γ_{avg}difference is about 0.5 and 2 dB at known CSI and unknown CSI schemes, respectively. The fact that the proposed structure performs almost independent of the atmospheric turbulence intensity is one of its advantages. Owing to this independence, eliminates the requirement of additional adaptive processing that adjusts system parameters to

$$
\begin{aligned}
P_{\mathrm{out}}(\gamma_{\mathrm{th}}) = 1 &- \sum_{k=0}^{N-1}\binom{N-1}{k}(-1)^k\frac{N}{k+1}\mathrm{e}^{-((k+1)\gamma_{\mathrm{th}}/\bar{\gamma}_{\mathrm{RF}})}\\
&\times\left[1-\frac{\xi^2 2^{\alpha+\beta-3}}{\pi\Gamma(\alpha)\Gamma(\beta)}G_{4,\,9}^{7,\,2}\left(\frac{(\alpha\beta\kappa)^2C\gamma_{\mathrm{th}}(k+1)}{16\bar{\gamma}_{\mathrm{FSO}}\bar{\gamma}_{\mathrm{RF}}}\middle|\begin{matrix}\psi_1\\ \psi_2\end{matrix}\right)\right]\\
&-\sum_{k=0}^{N-1}\binom{N-1}{k}(-1)^k\frac{N}{k+1}\mathrm{e}^{-((k+1)\gamma_{\mathrm{th}}/\bar{\gamma}_{\mathrm{RF}})}\,G_{0,\,2}^{2,\,0}\left(\frac{C\gamma_{\mathrm{th}}(k+1)}{\bar{\gamma}_{\mathrm{RF}}^2}\middle|\begin{matrix}-\\ 1,\,0\end{matrix}\right)\\
&+\sum_{k=0}^{N-1}\sum_{g=0}^{N-1}\binom{N-1}{k}\binom{N-1}{g}(-1)^{k+g}\frac{N^2}{(k+1)(g+1)}\mathrm{e}^{-\frac{(g+k+2)\gamma_{\mathrm{th}}}{\bar{\gamma}_{\mathrm{RF}}}}\\
&\times G_{0,\,2}^{2,\,0}\left(\frac{C\gamma_{\mathrm{th}}(k+1)}{\bar{\gamma}_{\mathrm{RF}}^2}\middle|\begin{matrix}-\\ 1,\,0\end{matrix}\right)\left[1-\frac{\xi^2 2^{\alpha+\beta-3}}{\pi\Gamma(\alpha)\Gamma(\beta)}G_{4,\,9}^{7,\,2}\left(\frac{(\alpha\beta\kappa)^2C\gamma_{\mathrm{th}}(k+1)}{16\bar{\gamma}_{\mathrm{FSO}}\bar{\gamma}_{\mathrm{RF}}}\middle|\begin{matrix}\psi_1\\ \psi_2\end{matrix}\right)\right]
\end{aligned}
\tag{39}
$$

$$
\begin{aligned}
P_{\mathrm{e}} = \frac{1}{2}\Bigg\{1 &- \sum_{k=0}^{N-1}\binom{N-1}{k}(-1)^k\frac{N}{k+1}\frac{1}{1+(k+1/\bar{\gamma}_{\mathrm{RF}})}\\
&\times\quad\left[1-\frac{\xi^2 2^{\alpha+\beta-3}}{\pi\Gamma(\alpha)\Gamma(\beta)}G_{5,\,9}^{7,\,3}\left(\frac{(\alpha\beta\kappa)^2C(k+1)}{16\bar{\gamma}_{\mathrm{FSO}}(\bar{\gamma}_{\mathrm{RF}}+k+1)}\middle|\begin{matrix}0,\,\psi_1\\ \psi_2\end{matrix}\right)\right]\\
&-\quad\sum_{k=0}^{N-1}\binom{N-1}{k}(-1)^k\frac{N}{k+1}\frac{1}{1+(k+1/\bar{\gamma}_{\mathrm{RF}})}\,G_{1,\,2}^{2,\,1}\left(\frac{C(k+1)}{\bar{\gamma}_{\mathrm{RF}}(\bar{\gamma}_{\mathrm{RF}}+k+1)}\middle|\begin{matrix}0\\ 1,\,0\end{matrix}\right)\\
&+\quad\sum_{k=0}^{N-1}\sum_{g=0}^{N-1}\binom{N-1}{k}\binom{N-1}{g}(-1)^{k+g}\frac{N^2}{(k+1)(g+1)}\frac{1}{1+(g+k+2/\bar{\gamma}_{\mathrm{RF}})}\\
&\times\quad\left[G_{1,\,2}^{2,\,1}\left(\frac{C(k+1)}{\bar{\gamma}_{\mathrm{RF}}(\bar{\gamma}_{\mathrm{RF}}+k+\mathrm{g}+2)}\middle|\begin{matrix}0\\ 1,\,0\end{matrix}\right)-\frac{\xi^2 2^{\alpha+\beta-3}}{\pi\Gamma(\alpha)\Gamma(\beta)}G_{1,\,0:0,\,2:4,\,9}^{1,\,0:2,\,0:7,\,2}\right.\\
&\times\quad\left.\left(\begin{matrix}1\\ -\\ 0,\,1\end{matrix}\middle|\begin{matrix}-\\ \psi_1\\ \psi_2\end{matrix}\middle|\begin{matrix}C(k+1)\\ \bar{\gamma}_{\mathrm{RF}}(\bar{\gamma}_{\mathrm{RF}}+k+g+2),\\ \frac{(\alpha\beta\kappa)^2C(g+1)}{16\bar{\gamma}_{\mathrm{FSO}}(\bar{\gamma}_{\mathrm{RF}}+k+\mathrm{g}+2)}\end{matrix}\right)\right]\Bigg\}
\end{aligned}
\tag{40}
$$

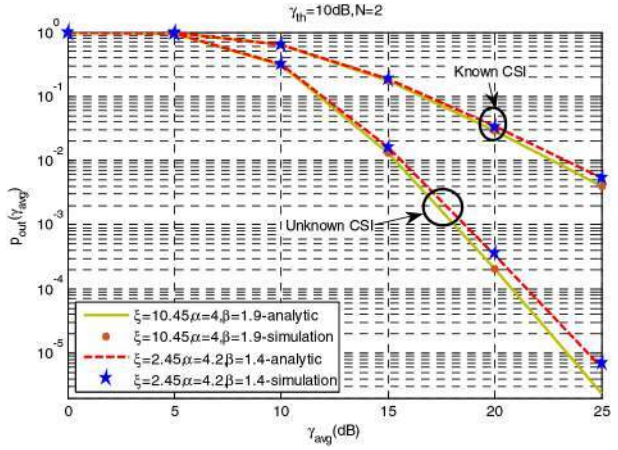

Fig. 3 *Outage probability of the proposed structure in terms of average SNR for moderate* ($\alpha = 4$, $\beta = 1.9$, $\xi = 10.45$) *and strong* ($\alpha = 4.2$, $\beta = 1.4$, $\xi = 2.45$) *atmospheric turbulence regimes, for both cases of known CSI and unknown CSI, number of users of* $N = 2$ *and* $\gamma_{\text{th}} = 10\,dB$

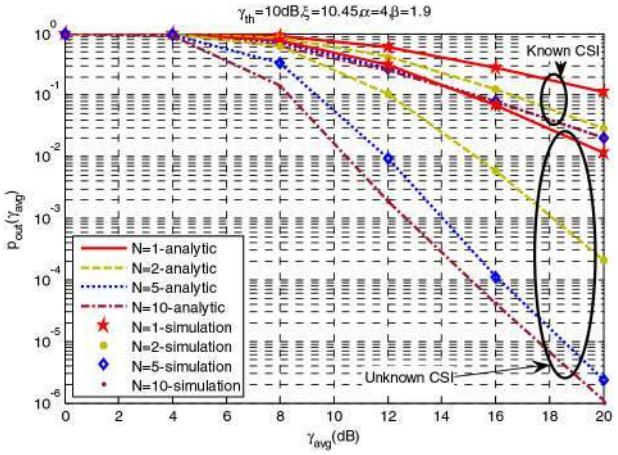

Fig. 4 *Outage probability of the proposed structure in terms of average SNR for the various number of users, for both cases of known CSI and unknown CSI, moderate atmospheric turbulence regime* ($\alpha = 4$, $\beta = 1.9$, $\xi = 10.45$) *and* $\gamma_{th} = 10\,dB$

maintain performance at various atmospheric turbulence intensities. Thereby cost, power consumption, complexity, and processing latency of the proposed system are greatly reduced. Unknown CSI scheme has better performance than known CSI scheme, and this is related to the constant parameter (C) used in unknown CSI scheme, which is adjusted manually by the operator. However, this improvement in the case of unknown CSI is obtained by consuming more power in an amplification block.

In Fig. 4, outage probability of the proposed structure is plotted in terms of average SNR for the various number of users for both cases of known CSI and unknown CSI, moderate atmospheric turbulence regime ($\alpha = 4$, $\beta = 1.9$, $\xi = 10.45$) and $\gamma_{\text{th}} = 10\,\text{dB}$. As can be seen, in both known CSI and unknown CSI schemes, system performance is strongly dependent on the number of users. Owing to the independence of first-hop RF paths, the probability of availability of all received signals is equal to the product of the probability of availability of individual paths. Hence, when the number of users decreases, in fact, the number of signals used for decision at the access point decreases. Thus, finding an available signal becomes easier. From this point of view, the proposed structure is powerful and cost-effective especially within the cells with a large number of users. Since without using additional processing or complexity, system performance becomes favourable even at low SNRs.

Dependence on the number of users in the case of known CSI is less than the unknown CSI. Since when CSI is available, the access point detects the received signal based on an adaptive threshold

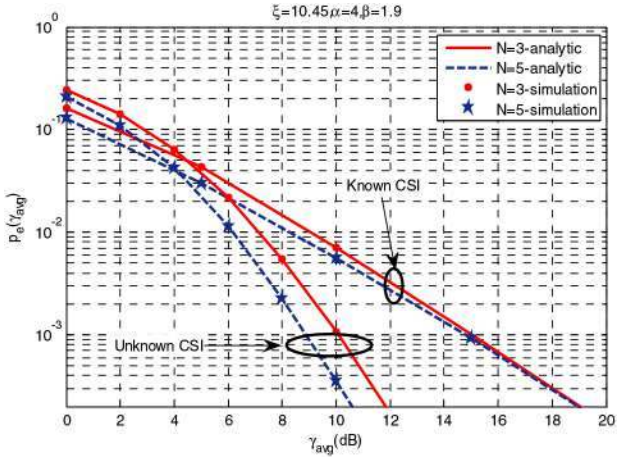

Fig. 5 *BER of the proposed structure in terms of average SNR for various numbers of users, for both cases of known CSI and unknown CSI and moderate atmospheric turbulence regime* ($\alpha = 4$, $\beta = 1.9$, $\xi = 10.45$)

and adjusts itself to the conditions. However, amplification by a fixed gain increases the performance difference between different numbers of users. Since noise and fading coefficients are also amplified.

In Fig. 5, BER of the proposed structure is plotted in terms of average SNR for various numbers of users, for both cases of known CSI and unknown CSI, and moderate atmospheric turbulence regime ($\alpha = 4$, $\beta = 1.9$, $\xi = 10.45$). It can be seen that at $\gamma_{\text{avg}} \leq 5\,\text{dB}$ known CSI scheme performs better than unknown CSI, but at $\gamma_{\text{avg}} \geq 5\,\text{dB}$, unknown CSI scheme has better performance. This is related to the constant parameter (C) in unknown CSI scheme, which is assumed to be unit ($C = 1$). If C was chosen smaller, then unknown CSI scheme would show better performance at all γ_{avg}.

It can be seen that at low γ_{avg}, the performance of both known CSI and unknown CSI schemes depends on the number of users within the cell, but at high γ_{avg}, this dependence decreases in the case of known CSI and increases in the case of unknown CSI.

In Fig. 6, BER of the proposed structure is plotted in terms of average SNR for moderate ($\alpha = 4$, $\beta = 1.9$, $\xi = 10.45$) and strong ($\alpha = 4.2$, $\beta = 1.4$, $\xi = 2.45$) regimes of gamma–gamma atmospheric turbulence with the effect of pointing error for both cases of known CSI and unknown CSI, and number of users of $N = 2$. As can be seen, there is little performance difference between moderate and strong atmospheric turbulence regimes. Therefore, the proposed system does not require adaptive processing or consuming much more power to maintain its performance. This is important especially for cells, which encounter frequent changes of atmospheric turbulence intensity during the day. In these areas, the frequent adaptation of system parameters does not work, and it may also cause more performance degrades. However, in the proposed system, performance maintains without additional processing or power consumption.

As can be seen, the main advantage of the proposed structure is its favourable performance even at low SNRs. This fact makes it suitable for power demand applications such as mobile communication systems, in which a small mobile battery supplies transmitter power.

In Fig. 7, BER of the proposed structure in terms of average SNR, for unknown CSI, strong atmospheric turbulence regime ($\alpha = 4$, $\beta = 1.9$), and $c = 1$. The purpose is to find out the improvement of adding a simple FSO transceiver on the performance of the system. Accordingly, three structures are compared: (i) RF users--(RF link)--access point--(RF link)-- base station; (ii) RF users--(RF link)--access point--(FSO link)-- base station; and (iii) RF users--(RF link)--access point--(FSO/RF link)--base station.

Consider the scenario, in which there are some users in the building, and they connect to an access point, the access point connects to the base station. The link between users and the access point is OK (it is in the building and everything is all right), but the

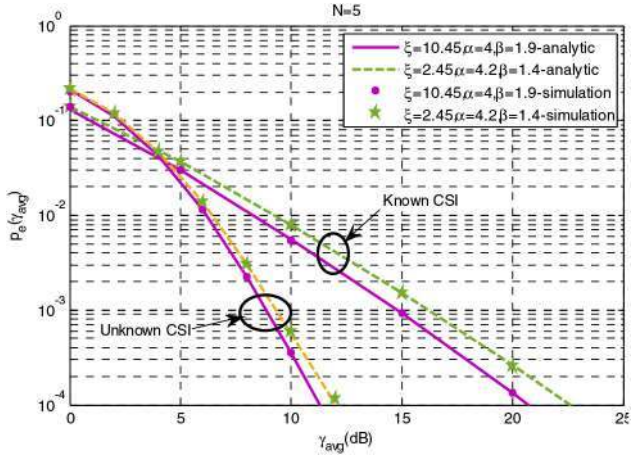

Fig. 6 *BER of the proposed structure in terms of average SNR for moderate* ($\alpha = 4$, $\beta = 1.9$, $\xi = 10.45$) *and strong* ($\alpha = 4.2$, $\beta = 1.4$, $\xi = 2.45$) *regimes of gamma–gamma atmospheric turbulence with the effect of pointing error for both cases of known CSI and unknown CSI, and number of users of* $N = 2$

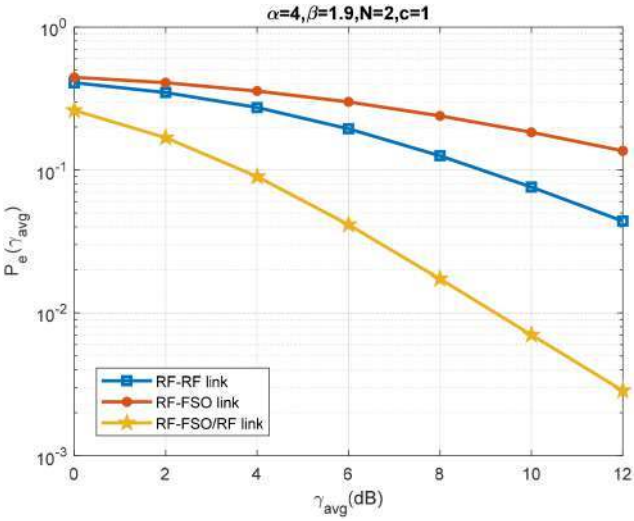

Fig. 7 *BER of the proposed structure in terms of average SNR, for unknown CSI, and strong atmospheric turbulence regime* ($\alpha = 4$, $\beta = 1.9$), *and* $c = 1$

link between access point and base station frequently encounters bad channel condition. So what are the solutions? Considering the worst-case scenario, effective solutions include increasing number of antennas, using huge coding, adding heavier equalisation/detection/processing etc. Although these might improve performance, but they have complexity, processing latency, power consumption etc., so they are not preferable in mobile communication, in which consumers expect satisfying low-cost communication.

However, this paper suggests to use a simple FSO transceiver (why?), simply because FSO and RF links complement each other, if one of them is in bad condition, the other one is in good condition. However, it has worth comparing the suggested system with previous paragraph systems. (i) The FSO transceiver is composed of a laser, and a photodetector, which is not as expensive as a complex equaliser, detector, or encoder, or many antennas etc. (ii) The FSO transceiver does not increase complexity and processing, so, it does not have latency. (iii) Laser consumes much less power than antenna, because its beam is directed naturally and does not waste anything; it has less power than complex processing, decoding, equalising etc.

As results indicate, the addition of a simple FSO transceiver presents a favourable performance even in the worst-case scenario (strong atmospheric turbulence considering pointing error). This suggestion has less cost, latency, and complexity compared with

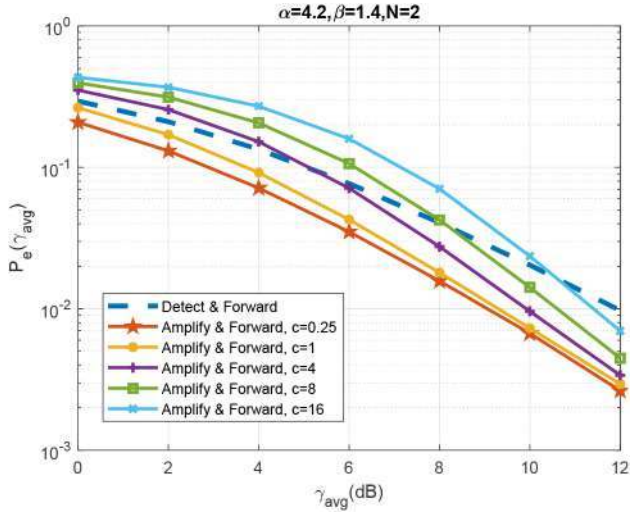

Fig. 8 *BER of the proposed structure in terms of average SNR, for both cases of known CSI and unknown CSI, for different values of C, for strong atmospheric turbulence regime* ($\alpha = 4$, $\beta = 1.9$)

addition of multiple-input–multiple-output, equaliser, coding etc. Only because FSO and RF naturally complement each other, e.g. in a situation that RF is disrupted completely, instead of using huge processing etc., could use a simple FSO transceiver, because FSO would work at that condition.

In Fig. 8, BER of the proposed structure is plotted in terms of average SNR, for both cases of known CSI and unknown CSI (for different values of C), for strong atmospheric turbulence regime ($\alpha = 4$, $\beta = 1.9$). One of the ambiguities the reader might encounter in the simulation results is the outperforming of unknown CSI scheme over known CSI scheme. For removing this ambiguity, should consider the definition of the amplification gain in unknown CSI scheme, in the paragraph after (12), $G^2 = 1/(C\sigma_{RF}^2)$. It is related to two parameters: a constant c and the inverse of SNR (signal power is assumed to be unit). Everything is related to these two parameters. The effects of these two parameters on the gain, and accordingly on the performance of the proposed structure can be seen in Fig. 8. As can be seen, at the low values of C (high gains), unknown CSI outperforms known CSI at all SNRs, but at high values of C (low gains), known CSI outperforms unknown CSI.

6 Conclusion

In this paper, a novel model is presented for hybrid FSO/RF communication system, in which an access point connects users within a building to the base station via a hybrid parallel FSO/RF link. FSO link has gamma–gamma atmospheric turbulence with the effect of pointing error and RF link has Rayleigh fading. Performance of the proposed system is investigated for both cases of known CSI and unknown CSI at the access point. For the first time, closed-form expressions are derived for BER and P_{out} of the proposed structure. MATLAB simulations verified the derived expressions.

In this work, for the first time, the effect of the number of users within the building on the performance of a dual-hop hybrid FSO/RF link is investigated at moderate-to-strong atmospheric turbulence. Performance of the system improves by increasing the number of users because the access point selects the user with the highest SNR. However, in the case of unknown CSI, this improvement is more. When CSI is available, system parameters can get adapted to the conditions; thus, the dependence on the number of users is low. However, unknown CSI scheme is more dependent because the selected signal is amplified by a fixed gain; the higher this gain, the bigger performance difference between various numbers of users. Communication systems which encounter fast and frequent changes in atmospheric turbulence intensity need the independent performance of atmospheric turbulence intensity. It is shown that there is little performance

difference between moderate and strong atmospheric turbulence regimes. The proposed system maintains performance without additional processing or power consumption and complexity, and also it offers favourable performance even at low SNRs. Therefore, it is economically affordable and particularly suitable for power demanding applications such as multi-user mobile communication systems.

7 References

[1] Trinh, P.V., Thang, T.C., Pham, A.T.: 'Mixed mmWave RF/FSO relaying systems over generalized fading channels with pointing errors', *IEEE Photonics J.*, 2017, **9**, (1), pp. 1–14

[2] Abadi, M.M., Ghassemlooy, Z., Zvanovec, S., *et al.*: 'Impact of channel link parameters and correlation on the performance of FSO systems with the differential signaling technique', *J. Opt. Commun. Netw.*, 2017, **9**, (2), pp. 138–148

[3] Ansari, I.S., Alouini, M.S., Yilmaz, F.: 'On the performance of hybrid RF and RF/FSO fixed gain dual-hop transmission systems'. 2013 Saudi Int. Electronics, Communications and Photonics Conf., Fira, Greece, April 2013, pp. 1–6

[4] Ai, D.H., Quang, D.T., Nam, N.N., *et al.*: 'Capacity analysis of amplify-and-forward free-space optical communication systems over atmospheric turbulence channels'. Seventh Int. Conf. Information Science and Technology (ICIST), Da Nang, Vietnam, 2017

[5] Saidi, H., Tourki, K., Hamdi, N.: 'DF dual-hop hybrid analysis of PSK modulation in performance RF/FSO system over gamma–gamma channel', Int. Symp. Signal, Image, Video and Communications (ISIVC), Tunis, Tunisia, 2016

[6] Chen, L., Wang, W., Zhang, C.: 'Multiuser diversity over parallel and hybrid FSO/RF links and its performance analysis', *IEEE Photonics J.*, 2016, **8**, pp. 1–9

[7] Mai, V.V., Pham, A.T.: 'Adaptive multi-rate designs for hybrid FSO/RF systems over fading channels'. Globecom Workshops (GC Wkshps), Austin, TX, USA, 2015, pp. 469–474

[8] Kolka, Z., Kincl, Z., Biolkova, V., *et al.*: 'Hybrid FSO/RF test link'. Fourth Int. Congress on Ultra Modern Telecommunications and Control Systems and Workshops (ICUMT), St Petersburg, Russia, 2012

[9] AbdulHussein, A., Oka, A., Nguyen, T.T., *et al.*: 'Rateless coding for hybrid free-space optical and radio-frequency communication', *IEEE Trans. Wirel. Commun.*, 2010, **9**, (3), pp. 907–913

[10] Zhang, W., Hranilovic, S., Shi, C.: 'Soft-switching hybrid FSO/RF links using short-length raptor codes: design and implementation', *IEEE J. Sel. Areas Commun.*, 2009, **27**, (9), pp. 1698–1708

[11] Makki, B., Svensson, T., Pearce, M. B., *et al.*: 'Performance analysis of RF-FSO multi-hop networks'. IEEE Wireless Communications and Networking Conf. (WCNC), San Francisco, CA, USA, 2017, pp. 1–6

[12] Amirabadi, M.A., Vakili, V.T.: 'A novel hybrid FSO/RF communication system with receive diversity', arXiv preprint arXiv:1802.07348, February 2018

[13] Amirabadi, M.A.: 'An optimization problem on the performance of FSO communication system', arXiv preprint arXiv:1902.10043, 2019

[14] Amirabadi, M.A., Vakili, V.T.: 'A new optimization problem in FSO communication system', *IEEE Commun. Lett.*, 2018, **22**, (7), pp. 1442–1445

[15] Soleimani-Nasab, E., Uysal, M.: 'Generalized performance analysis of mixed RF/FSO cooperative systems', *IEEE Trans. Wirel. Commun.*, 2016, **15**, (1), pp. 714–727

[16] Kumar, K., Borah, D.K.: 'Quantize and encode relaying through FSO and hybrid FSO/RF links', *IEEE Trans. Veh. Technol.*, 2015, **64**, (6), pp. 2361–2374

[17] Boluda-Ruiz, R., García-Zambrana, A., Castillo-Vázquez, B., *et al.*: 'MISO relay-assisted FSO systems over gamma–gamma fading channels with pointing errors', *IEEE Photonics Technol. Lett.*, 2016, **28**, (3), pp. 229–232

[18] Boluda-Ruiz, R., García-Zambrana, A., Castillo-Vázquez, B., *et al.*: 'Ergodic capacity analysis of decode-and-forward relay-assisted FSO systems over alpha–mu fading channels considering pointing errors', *IEEE Photonics J.*, 2016, **8**, (1), pp. 1–11

[19] Anees, S., Bhatnagar, M. R.: 'Performance of an amplify-and-forward dual-hop asymmetric RF-FSO communication system', *IEEE/OSA J. Opt. Commun. Netw.*, 2015, **7**, (2), pp. 124–135

[20] Zhang, J., Dai, L., Zhang, Y., *et al.*: 'Unified performance analysis of mixed radio-frequency/free-space optical dual-hop transmission systems', *J. Lightwave Technol.*, 2015, **33**, (11), pp. 2286–2293

[21] Jing, Z., Shang-hong, Z., Wei-hu, Z., *et al.*: 'Performance analysis for mixed FSO/RF Nakagami-*m* and exponentiated Weibull dual-hop airborne systems', *Opt. Commun.*, 2017, **392**, pp. 294–299

[22] Zedini, E., Ansari, I.S., Alouini, M.S.: 'Performance analysis of mixed Nakagami-*m* and gamma–gamma dual-hop FSO transmission systems', *IEEE Photonics J.*, 2015, **7**, (1), pp. 1–20

[23] Amirabadi, M.A., Vakili, V.T.: 'Performance analysis of hybrid FSO/RF communication systems with Alamoudi coding or antenna selection', arXiv preprint arXiv:1802.07286, February 2018

[24] Kong, L., Xu, W., Hanzo, L., *et al.*: 'Performance of a free-space-optical relay-assisted hybrid RF/FSO system in generalized *M*-distributed channels', *IEEE Photonics J.*, 2015, **7**, (5), pp. 1–19

[25] Anees, S., Bhatnagar, M.R.: 'Performance of an amplify-and-forward dual-hop asymmetric RF–FSO communication system', *J. Opt. Commun. Netw.*, 2015, **7**, (2), pp. 124–135

[26] Jamali, V., Michalopoulos, D.S., Uysal, M., *et al.*: 'Mixed RF and hybrid RF/FSO relaying'. 2015 IEEE Globecom Workshops (GC Wkshps) IEEE, 2015, December, pp. 1–6

[27] Djordjevic, G., Petkovic, M., Cvetkovic, A., *et al.*: 'Mixed RF/FSO relaying with outdated channel state information', *IEEE J. Sel. Areas Commun.*, 2015, **33**, pp. 1935–1948

[28] Miridakis, N.I., Matthaiou, M., Karagiannidis, G.K.: 'Multiuser relaying over mixed RF/FSO links', *IEEE Trans. Commun.*, 2014, **62**, (5), pp. 1634–1645

[29] Zedini, E., Soury, H., Alouini, M.S.: 'On the performance analysis of dual-hop mixed FSO/RF systems', *IEEE Trans. Wirel. Commun.*, 2016, **15**, (5), pp. 3679–3689

[30] Zedini, E., Soury, H., Alouini, M. S.: 'On the performance of dual-hop FSO/RF systems'. 2015 Int. Symp. Wireless Communication Systems (ISWCS) IEEE, Brussels, Belgium, August 2015, pp. 31–35

[31] Lee, E., Park, J., Han, D., *et al.*: 'Performance analysis of the asymmetric dual-hop relay transmission with mixed RF/FSO links', *IEEE Photonics Technol. Lett.*, 2011, **23**, (21), pp. 1642–1644

[32] Samimi, H., Uysal, M.: 'End-to-end performance of mixed RF/FSO transmission systems', *J. Opt. Commun. Netw.*, 2013, **5**, (11), pp. 1139–1144

[33] Bag, B., Das, A., Chandra, A., *et al.*: 'Capacity analysis for Rayleigh/gamma–gamma mixed RF/FSO link with fixed-gain AF relay', *IEICE Trans. Commun.*, 2017, **100**, (10), pp. 1747–1757

[34] Zedini, E., Soury, H., Alouini, M.S.: 'Dual-hop FSO transmission systems over gamma–gamma turbulence with pointing errors', *IEEE Trans. Wirel. Commun.*, 2017, **16**, (2), pp. 784–796

[35] Varshney, N., Puri, P.: 'Performance analysis of decode-and-forward-based mixed MIMO-RF/FSO cooperative systems with source mobility and imperfect CSI', *J. Lightwave Technol.*, 2017, **35**, (11), pp. 2070–2077

[36] Sharma, P.K., Bansal, A., Garg, P.: 'Relay assisted bi-directional communication in generalized turbulence fading', *J. Lightwave Technol.*, 2015, **33**, (1), pp. 133–139

[37] Sharma, P.K., Garg, P.: 'Bi-directional decode-XOR-forward relaying over *M*-distributed free-space optical links', *IEEE Photonics Technol. Lett.*, 2014, **26**, (19), pp. 1916–1919

[38] Wang, P., Cao, T., Guo, L., *et al.*: 'Performance analysis of multihop parallel free-space optical systems over exponentiated Weibull fading channels', *IEEE Photonics J.*, 2015, **7**, (1), pp. 1–17

[39] Kashani, M.A., Uysal, M.: 'Outage performance of FSO multi-hop parallel relaying'. Signal Processing and Communications Applications Conf. IEEE, Mugla, Turkey, April 2012, pp. 1–4

[40] Kashani, M.A., Uysal, M.: 'Outage performance and diversity gain analysis of free-space optical multi-hop parallel relaying', *IEEE/OSA J. Opt. Commun. Netw.*, 2013, **5**, (8), pp. 901–909

[41] Najafi, M., Jamali, V., Schober, R.: 'Optimal relay selection for the parallel hybrid RF/FSO relay channel: non-buffer-aided and buffer-aided designs', *IEEE Trans. Commun.*, 2017, **65**, (7), pp. 2794–2810

[42] Amirabadi, M.A., Vakili, V.T.: 'Performance comparison of two novel relay-assisted hybrid FSO/RF communication systems', arXiv preprint arXiv:1802.07335, February 2018

[43] Rakia, T., Yang, H.C., Gebali, F., *et al.*: 'Power adaptation based on truncated channel inversion for hybrid FSO/RF transmission with adaptive combining', *IEEE Photonics J.*, 2015, **7**, (4), pp. 1–12

[44] Wolfram, The Wolfram functions site. Available at http://functions.wolfram.com/

[45] Bhatnagar, M.R., Ghassemlooy, Z.: 'Performance analysis of gamma–gamma fading FSO MIMO links with pointing errors', *J. Lightwave Technol.*, 2016, **34**, (9), pp. 2158–2169

[46] Kazemi, H., Uysal, M., Touati, F., *et al.*: 'Outage performance of multi-hop hybrid FSO/RF communication systems'. Fourth Int. Workshop on Optical Wireless Communications (IWOW), Istanbul, Turkey, September 2015, pp. 83–87

[47] Ansari, I.S., Al-Ahmadi, S., Yilmaz, F., *et al.*: 'A new formula for the BER of binary modulations with dual-branch selection over-*K* composite generalized fading channels', *IEEE Trans. Commun.*, 2011, **59**, (10), pp. 2654–2658